Cell. Mol. Life Sci. (2015) 72:2961–2971
DOI 10.1007/s00018-015-1878-2

Cellular and Molecular Life Sciences

RESEARCH ARTICLE

The HERC1 E3 Ubiquitin Ligase is essential for normal development and for neurotransmission at the mouse neuromuscular junction

S. Bachiller · T. Rybkina · E. Porras-García · E. Pérez-Villegas · L. Tabares · J. A. Armengol · A. M. Carrión · R. Ruiz

Received: 18 November 2014 / Revised: 15 February 2015 / Accepted: 27 February 2015 / Published online: 8 March 2015

Abstract The ubiquitin–proteasome system (UPS) plays a fundamental role in protein degradation in neurons, and there is strong evidence that it fulfills a key role in synaptic transmission. The aim of the present work was to study the implication of one component of the UPS, the HERC1 E3 Ubiquitin Ligase, in motor function and neuromuscular transmission. The *tambaleante* (*tbl*) mutant mouse carries a spontaneous mutation in HERC1 E3 Ubiquitin Ligase, provoking an ataxic phenotype that develops in the second month of life. Our results show that motor performance in mutant mice is altered at postnatal day 30, before the cerebellar neurodegeneration takes place. This defect is associated with by: (a) a reduction of the motor end-plate area, (b) less efficient neuromuscular activity in vivo, and (c) an impaired evoked neurotransmitter release. Together, these data suggest that the HERC1 E3 Ubiquitin Ligase is fundamental for normal muscle function and that it is essential for neurotransmitter release at the mouse neuromuscular junction.

Keywords Vesicle · Proteasome · Electromyography (EMG) · Ready releasable pool (RRP) · Synapse · Intracellular recording

Electronic supplementary material The online version of this article (doi:10.1007/s00018-015-1878-2) contains supplementary material, which is available to authorized users.

S. Bachiller · T. Rybkina · E. Porras-García · E. Pérez-Villegas · J. A. Armengol · A. M. Carrión · R. Ruiz (✉)
Department of Physiology, Anatomy and Cellular Biology, University of Pablo de Olavide, Carretera de Utrera Km 1, 41013 Seville, Spain
e-mail: rruizlaza@upo.es

L. Tabares
Department of Medical Physiology and Biophysics, University of Seville, Seville, Spain

J. A. Armengol
School of Medicine, University of Cartagena de Indias, Cartagena, Colombia

Introduction

The ligation of ubiquitin molecules to proteins is part of a key degradation pathway that strongly influences their turnover. Protein ubiquitination is the result of a cascade of catalytic reactions driven by the ubiquitin–proteasome system (UPS) involving three main groups of enzymes: E1 (ubiquitin-activating enzyme), E2 (ubiquitin-conjugating enzyme), and E3 (ubiquitin-protein ligase) (reviewed by [1, 2]). Several studies have revealed the fundamental role of the neuronal UPS in maintaining the homeostasis of synapses [1–4]. In fact, altering the protein degradation system has been related to neurodegenerative diseases like spinal and bulbar muscular atrophy (SBMA), X-spinal muscular atrophy [5–8], as well as Alzheimer's, Parkinson's, and Huntington's diseases [1, 9–12].

The localization of the UPS at synapses, and its implication in synaptic development, maintenance, and plasticity, has been investigated in invertebrates and vertebrates (for review see [1]). Recent studies show that the UPS plays a key role in neurotransmission at the neuromuscular junction [4, 13, 14]. However, despite the wealth of evidence that the UPS participates in physiological and pathological events in the nervous system, the specific role fulfilled by the different UPS proteins is on the whole unknown. Thus, it is important to better understand how UPS activity affects the behavior of synapses.

The HERC 1 (HECT domain and RCC1 domain) E3 Ubiquitin Ligase is a component of the UPS. It has been reported that the Gly483Glu substitution within this protein

induces protein overexpression and is responsible for the *tambaleante* (*tbl*) phenotype in mice [15]. This phenotype is characterized by a severe ataxia uncoordinated gait, irregular hindlimb posture, and trembling [16–18], and it is associated with progressive Purkinje cell (PC) degeneration that first becomes obvious at about 2 months of age, deteriorating thereafter.

Here, we have studied *tambaleante* mutant mice to determine how the HERC1 E3 Ubiquitin Ligase participates in motor function and neuromuscular transmission. By performing electromyography in vivo and through the intracellular recording of postsynaptic muscle potentials *ex vitro*, we demonstrate that HERC1 malfunction produces motor defects prior to the manifestation of the ataxia phenotype and cerebellar cell loss. Hence, this ligase appears not only to be essential for PCs but also for synaptic activity at the neuromuscular junction (NMJ).

Materials and methods

Animal model

Tambaleante mice were kindly provided by Dr. Jose Luis Rosa (Department of Ciències Fisiològiques II, Facultat de Medicina, Universitat de Barcelona, Spain) and the experimental mice were obtained by breeding pairs of *tbl* carrier mice. Wild-type and mutant mice (*tbl/tbl*) were genotyped by PCR as described previously [15] and the control mice used were age-matched littermates of the mutants. All experiments were performed according to current Spanish legislation RD 53/2013 governing experimental animal care (BOE 08/02/2013).

Motor function tests

To habituate mice to the rotarod (Ugo Basile Biological Research Apparatus), the animals were placed on the roller at a speed of 20 rpm until they could remain on it for one minute without falling off. To assay motor coordination, animals were then tested at a rotational speed of 20 rpm, accelerating to 60 rpm in increments of 5 rpm, and quantifying the number of falls at each increase in speed. Forelimb muscle strength was measured using Digital Force Gauges (Chatillon DFE AMETEK), repeating the measurement five times in each experimental group.

Electrophysiological analysis of the *medial gastrocnemius* (MG) muscle in *tbl* mice

Compound muscular action potentials (CMAPs) were recorded in anesthetized mice (tribromethanol 2 %, 0.15 ml/10 g body weight, i.p.) as described previously [19–21]. Briefly, the recording needle electrode was placed into the medial part of the MG muscle and the reference electrode was situated at the base of the fifth phalanx. A ground electrode was also placed at the base of the tail, and stimulating needle electrodes were placed at the sciatic notch and the head of the fibula. Stimulation protocols of supramaximal current pulses (0.05 ms duration, 5–10 mA amplitude) were applied as a short train of 10, 50, and 100 Hz pulses generated by an isolated pulse stimulator (Pulse Train Stimulator Cibertec cs-20). The outputs recorded were differentially amplified (P511 AC Amplifier Astro-Med, INC), digitally acquired at 10,000 samples/s (CED 1401 Plus; Cambridge Electronic Designed, Cambridge, UK) and stored on a computer for later analysis. The analysis consisted of measuring the amplitude from the positive to the negative peak of the CMAPs recorded during a train of stimuli, normalizing the amplitude to the first response.

Muscle preparation for intracellular recording

Mice were anesthetized with tribromethanol as above and sacrificed by exsanguination. The *Levator Auris Longus* (*LAL*) muscle was dissected out with its nerve branches intact and pinned to the bottom of a 2 ml chamber on a bed of cured silicone rubber (Sylgard, Dow Corning). These preparations were perfused continuously with the following solution (in mM):125 NaCl, 5 KCl, 2 $CaCl_2$, 1 $MgCl_2$, 25 $NaHCO_3$, and 30 glucose. This solution was continuously gassed with 95 % O_2 and 5 % CO_2 to maintain its pH at 7.35, and recordings were obtained at room temperature (22–23 °C).

Ex vivo electrical stimulation and intracellular recording

The nerve was stimulated using a suction electrode, applying 0.2 ms square-wave pulses with a 2–40 V amplitude and variable frequency (0.5–100 Hz). Evoke end-plate potentials (EPPs) and miniature EPPs (mEPPs) were recorded as described previously [20, 22–24]. Muscle contractions were blocked with μ-conotoxin GIIIB (2–4 μM; Alomone Labs), a specific blocker of skeletal muscle voltage-gated sodium channels.

Intracellular recording analysis

The mean EPP and mEPP amplitudes recorded at each NMJ were normalized linearly to a −70 mV resting membrane potential and the EPPs were corrected for non-linear summation [25]. Quantal content (QC) was estimated by the direct method, which consists of simultaneously recording mEPPs and EPPs (0.5 Hz nerve

stimulation) and then calculating the ratio: QC = average peak EPP/average peak mEPP. The readily releasable pool (RRP) size was estimated as reported previously [26]. Briefly, the QCs obtained during a train were plotted against the cumulative number of quanta and the RRP was estimated by back-extrapolation from the linear portion of the curve to the x-axis intercept. The x-intercept gives an estimate of RRP based upon the assumption of negligible mobilization into the RRP [27, 28].

Immunohistochemistry

To analyze Purkinje cells (PCs), we followed the protocol described previously [29]. Briefly, control and *tbl* mice were sacrificed with an overdose of pentobarbital (80 mg/kg i.p.) and perfused intracardially with 4 % paraformaldehyde in phosphate-buffered saline (PBS). The cerebellum was dissected out and post-fixed by immersion in 4 % fresh fixative solution for 24 h at 4 °C. The tissue was then cryoprotected in 30 % sucrose-PBS at 4 °C until it sank, and coronal cerebellar cryotome section (30 µm thick) was processed for free-floating immunohistochemistry using a rabbit polyclonal antiserum against calbindin (1:4,000; Swant).

Immunofluorescence

Whole-mount *LAL, MG,* and *TVA (Transversus Abdominis)* muscles were incubated for 30 min in 4 % paraformaldehyde and immunostained as described previously [30]. Briefly, the muscles were bathed in 0.1 M glycine in PBS for 30 min, permeabilized with 1 % (v/v) Triton X-100 in PBS for 1 h, and then incubated in 5 % (w/v) BSA, 1 % Triton X-100 in PBS for 1 h. The tissue was then incubated overnight at 4 °C with the primary antibodies of interest (see below) and the following day, the muscles were rinsed for 1 h in PBS containing 0.05 % Triton X-100. After incubating for 1 h with the corresponding secondary antibodies (1:500; Alexa antibodies, Invitrogen) and 10 ng/ml rhodamine-BTX (Sigma Aldrich), and rinsing again with PBS containing 0.05 % Triton X-100 for 90 min, the muscles were mounted in Glycerol 50 % for visualization. Presynaptic terminals were labeled with antibodies against synaptophysin (1:500) and neurofilaments (NF; 1:500) (Santa Cruz).

Image acquisition and analysis

Fixed muscles were examined on an upright Leica DM 2500 confocal laser scanning microscope. During image acquisition, an alternating sequence of laser pulses was used to activate the different fluorescent probes. Images were taken using a 63× oil-immersion objective with a numerical aperture of 1.3. Images from wild-type and mutant littermates were obtained under similar conditions (laser intensities and photomultiplier voltages), and usually on the same day. Morphometric analysis of the fluorescently labeled structures was performed offline with Fiji ImageJ (W. Rasband, National Institutes of Health). Endplate and synaptic vesicle (SV) areas were determined automatically by defining outline masks based on brightness thresholds from maximal projected confocal images [30].

Statistical analysis

The results were analyzed with the SPSS package for Windows and unless otherwise stated, the data represent the mean ± SEM values. The *tambaleante* and control samples were compared using the Student's *t* test (two tailed) and a p value <0.05 was considered statistically significant. N = number of mice, n = number of NMJ or number of fibers. All the data represent the analysis of at least three animals per genotype as previously performed [31].

Results

Age-dependent motor function impairment in *tambaleante* mutant mice

During the first month of life, the body weight of *tbl* mutant mice was the same as their wild-type littermates but from this age onwards (postnatal day 30, P30), the homozygous mutants were easily distinguished from their wild-type and heterozygous littermates through their lower body weight (Fig. 1a). In addition, the motor performance of the mutant mice was also altered from 5 weeks of age onwards, as measured during rotarod assays (Fig. 1b). This test requires both strength and motor coordination, so we also measured the animal's forelimb strength using a grip strength test. The *tbl* mutant mice older than P30 had less strength in their forelimbs than age-matched control mice (Fig. 1c). The ataxia phenotype was first evident in the *tbl* mice at around 2 months of age, together with PC loss [15], although no morphological differences were evident in PCs between P30 *tbl* and control littermates (Fig. 1d). Thus, ours results suggest that *tbl* mice present a motor deficit prior to PC loss.

High frequency-induced neuromuscular depression is increased in *tambaleante* mutant mice at P30 and P120

The electrical neuromuscular properties of the *tbl* mice were studied in vivo by performing electromyography

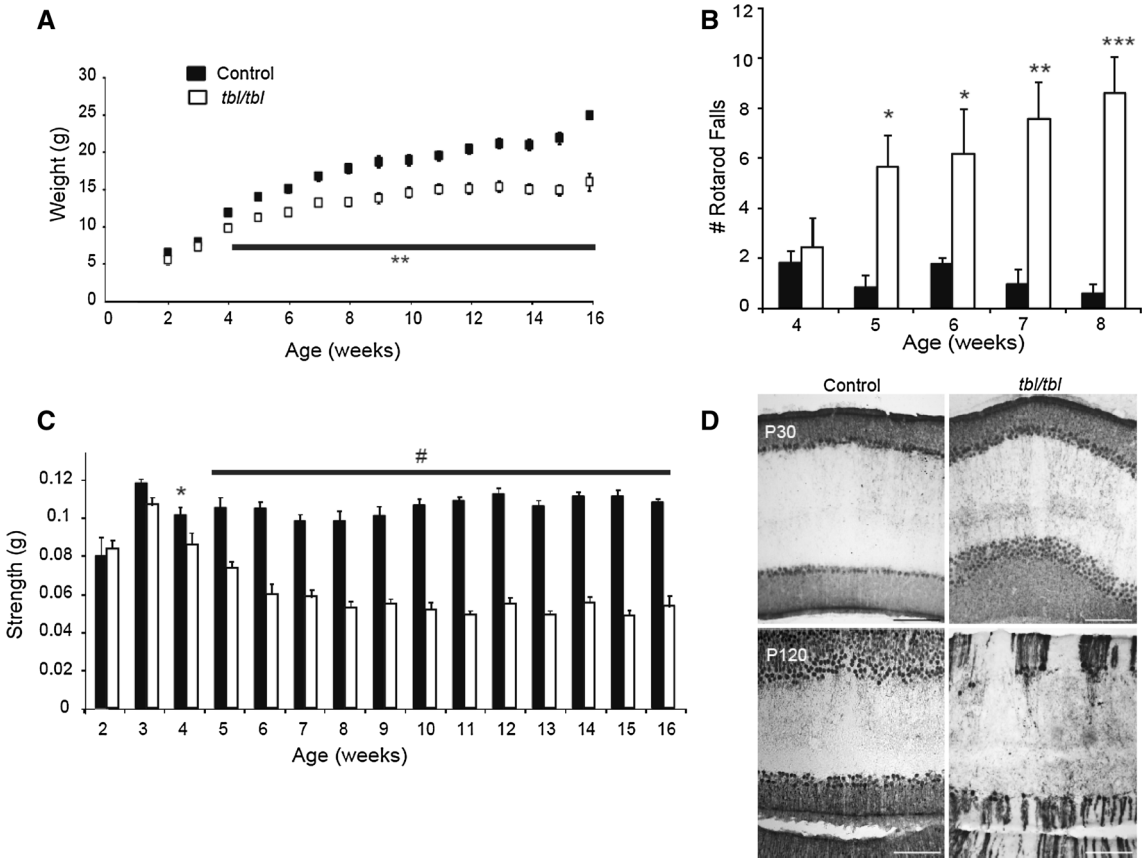

Fig. 1 Impaired motor strength and coordination in the *tambaleante* (*tbl*) mutant mice. **a** Body weight in mutant and control mice measured during the first 16 weeks of life ($N = 12$ mice per study group). **b** The number of falls from the rotarod increases in *tambaleante* mice from the fifth week of age ($N = 7$ mice in control group and $N = 9$ in *tambaleante*). **c** Forelimb strength was measured with a grip strength meter ($N = 12$ mice per study group). **d** Coronal sections staining with Anti-Calbindin in a control and *tambaleante* mouse cerebellum aged 1 and 4 months old: $^{*}p < 0.05$, $^{**}p < 0.005$; $^{***}p < 0.0005$; $^{\#}p < 0.00005$

(EMG) on the *medial gastrocnemius* (*MG*) muscle at P15 (Fig. 2a), P30 (Fig. 2b) and P120 (Fig. 2c), using short-train stimuli at different frequencies. At P30, the depression at the end of a train of 30 stimuli at 100 Hz was higher in *tbl* mutant than in the wild-type mice when measured by normalization of the CMAP amplitude (Control: 10.26 ± 3.9 %, $N = 8$ and *tbl*: 30.78 ± 6.8 %, $N = 4$, $p < 0.037$), evidence of reduced neuromuscular function in the *tbl* mutant mice at this age. No such defect was found at lower stimulation frequencies (10 and 50 Hz, Fig. 2b, right panel). Impaired motor function persisted at four months of age in mutant mice, but surprisingly these differences were no bigger than in the one-month-old *tbl* mice (the depression at the end of the train in 4-month-old *tbl* mutant mice was 35.64 ± 2.5 %, $N = 11$: $p = 0.27$ in comparison with depression at the end of the train in P30 *tbl* mice). However, there were significant differences between *tbl* mice and their control 4-month-old littermates not only at 100 Hz (control: 27.79 ± 2.8 %, $N = 9$: $p < 0.024$) but also at 50 Hz stimulation (*tbl:* 15.07 ± 1.8 %, $N = 11$ and Control: 7.15 ± 3.1 %, $N = 9$, Fig. 2c: $p < 0.037$). At P15, we found no differences in motor function in the EMG recordings (Fig. 2a), suggesting that impaired muscle neurotransmission was correlated with deficient grip strength and motor coordination. Together, these data show that impaired motor function is evident in *tbl* mutant mice from 30 days of age and that it persists over time.

Morphological alterations to the medial gastrocnemius neuromuscular junction in *tambaleante* mutant mice

We looked for possible morphological changes to the *MG* muscle at P30 in *tbl* mice to verify whether the altered EMG observed was accompanied by changes at the NMJ. When the size of the postsynaptic area was estimated by labeling nicotinic receptors with α-bungarotoxin-rhodamine, it was smaller in the mutants than in the controls at all ages studied (~32, ~24 and 18 % smaller at P15 ($p = 0.0000007$), P30 ($p < 0.000007$) and P120 ($p < 0.01$), respectively: Fig. 3a, b). Thus, the alterations to the EMG observed were accompanied by morphological changes at the synapse. Interestingly, the decrease in NMJ

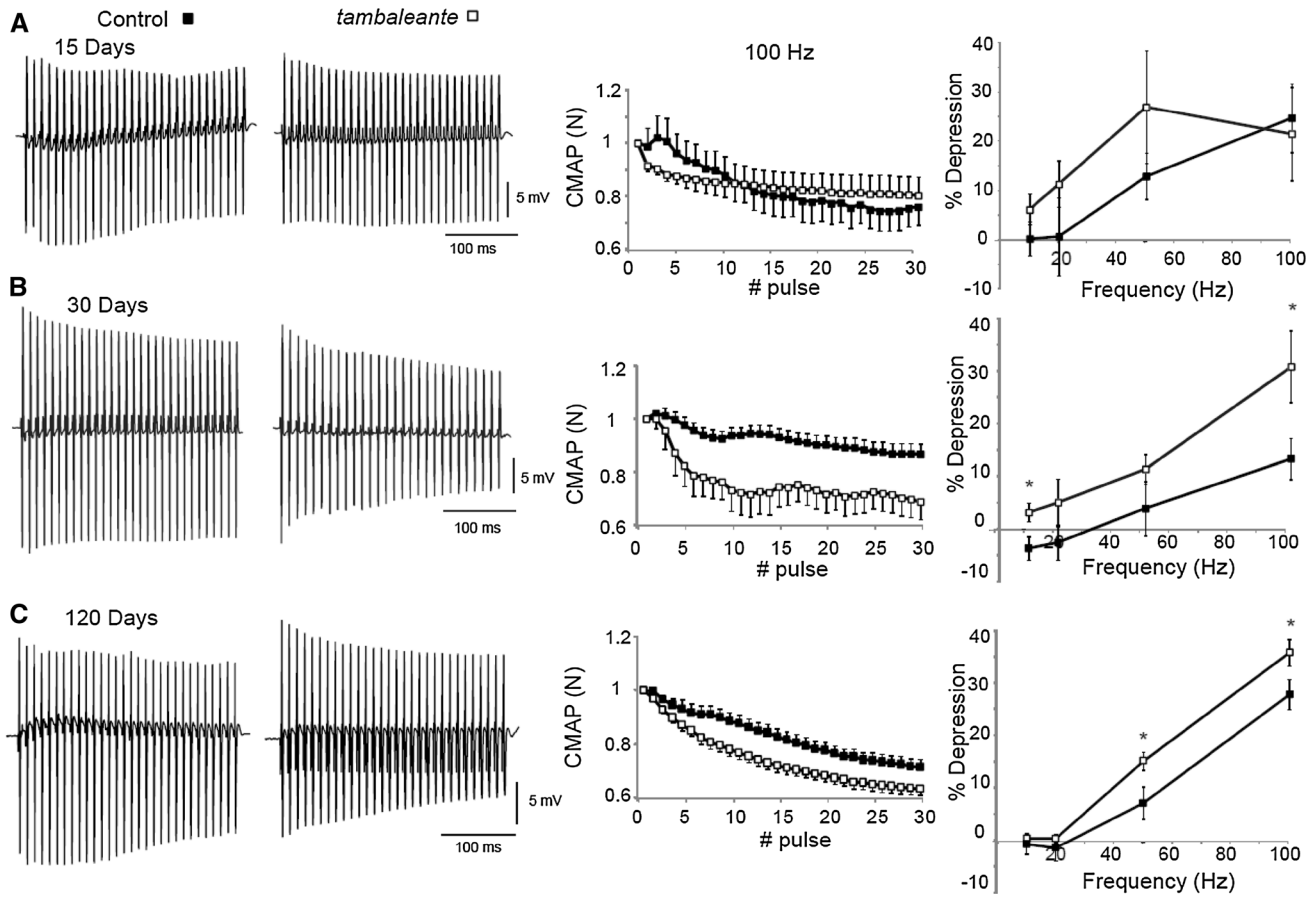

Fig. 2 EMG measurements of CMAP amplitudes in the *MG* of control and *tambaleante* mice reveal reduced neurotransmission efficacy in the *tbl* mice at postnatal day 30 and 120. Representative recordings during a train of stimuli at 100 Hz in a control and *tbl* mouse on postnatal days 15 ($N = 5$ mice per study group), 30 ($N = 8$ mice in control group and $N = 4$ in *tbl*) and 120 ($N = 9$ mice in control group and $N = 11$ in *tbl*). Depression of CMAP amplitudes (normalized to the first response) during a train of stimuli of 300 ms at 100 Hz in control and mutant mice at all the ages studied. **a**–**c** Relative depression of the CMAP amplitudes at the quasi steady-state level for stimulation frequencies from 10 to 100 Hz: $*p < 0.05$

postsynaptic area appeared since P15, before the onset of the functional impairment characterized by EMG, indicative of altered NMJ development.

The neuromuscular junction of fast- and slow-twitch muscle fibers is morphological altered in *tambaleante* mutant mice

The *MG* is a mixed muscle with about 50 % slow-twitch type muscle fibers and 50 % fast-twitch fibers. Thus, we assessed whether the alterations to the NMJ were restricted to a particular muscle fiber type in *tbl* mice. As models of fast- and slow-twitch muscles, the *levator auris longus* (*LAL*) and *Transversus Abdominis* (*TVA*) muscle were immunostained with an antibody against neurofilaments and synaptophysin to label the presynaptic compartment, and with α-bungarotoxin-rhodamine to label postsynapses in P15 control and *tbl* littermates. In the *tbl LAL* muscle, there was a ∼23 and 29 % decrease in labeling in the vesicular and postsynaptic areas, respectively, with respect to the control mice (Fig. 4a–c). Similar results were observed in the *TVA* muscle, with a significant decrease in the vesicular and postsynaptic areas of the *tbl* mice ∼11 and ∼29 percent lower than in control mice (Fig. 4d–f), suggesting that both types of muscle fibers are affected similarly in the *tbl* mice. These vesicular and postsynaptic differences persisted, as witnessed when a similar morphological study was performed on the LAL muscle from animals aged from P15 to four months of age (Supplementary Figure 1). Interestingly, the size of the estimated areas increased over time in both control and *tbl* mice but nevertheless, the significant difference in the vesicle and postsynaptic area was maintained. For example, from P15 to P120 the increment in vesicular area was ∼136 % in mutants and ∼119 % in controls, furthermore during the same period the postsynaptic area increased ∼136 and ∼111 %, respectively.

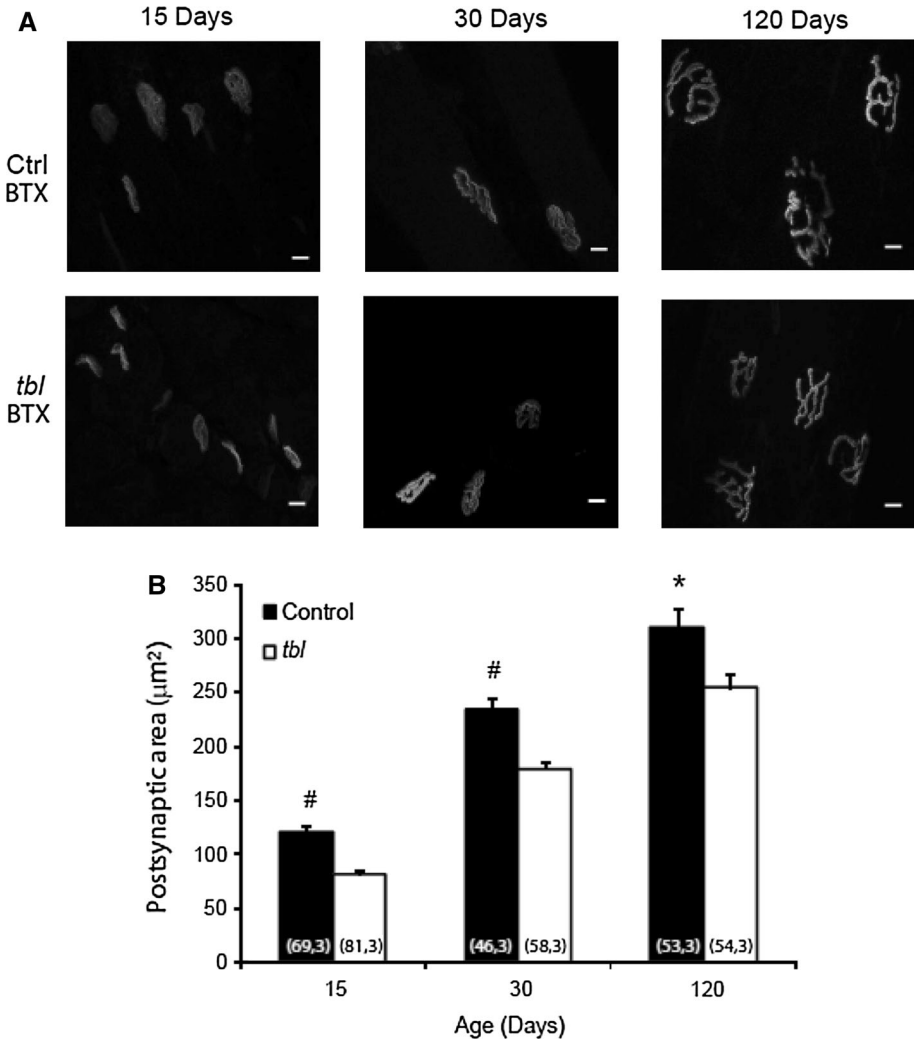

Fig. 3 BTX area in *MG* motor terminals of *tbl* mice is smaller than in control littermates at P15, P30 and P120. **a** Representative *en face* views of the neuromuscular junction (NMJ) from the *MG* muscle stained with BTX-Rho (*gray*) at P15, P30 and P120. Images are *Z*-stack projections and the *scale bar* 20 μm. **b** The mean postsynaptic areas at all ages studied: $^{*}p < 0.05$; $^{\#}p < 0.00005$ [(*n*, *N*), *n* number of NMJ, *N* number of mice]

Impairment in evoke neurotransmitter release in neuromuscular junction of *tambaleante* mutant mice

To study the effect of the HERC1 mutation on neurotransmitter release, we obtained intracellular recordings from the *LAL* muscle of two-month-old mice. We first recorded impaled muscle fibers to measure the amplitude of mEPPs from control and *tambaleante* mutant mice. The rank sum test indicated that the median mEPP amplitude in mutant fibers (1.51 mV) was not statistically different from that of the controls (1.94 mV, $p = 0.294$: Fig. 5a). We then examined evoked neurotransmitter release at motor terminals of the LAL muscle in response to a single action potential. The mean size of the EPPs in control animals was larger than in their *tbl* littermates (mutants: 27.60 ± 2.49 mV; controls: 41.98 ± 4.81 mV, $p < 0.01$: Fig. 5b) and so, we also compared the QC defined as the number of vesicles that fuse per action potential. The QC was lower in mutants than in control littermates (compare 16.59 ± 1 and 23.34 ± 2.27 for *tbl* and control mice respectively, $p < 0.008$: Fig. 5c). Together, these data indicate that the morphological alterations found may be associated with functional impairment.

Short-term plasticity is preserved in the neuromuscular junction of *tambaleante* mutant mice

One possible explanation for the decline in evoked neurotransmitter release could be the inability to maintain vesicle release during a train of stimuli [32]. To examine this possibility, we compared the EPP amplitudes in control and mutant fibers during a train of 10 stimuli at different stimulation frequencies (10, 20, 50 and 100 Hz), normalizing the EPP amplitudes recorded to the first response (Fig. 6a). No differences in short-term plasticity were found between controls and *tbl* mice at any stimulation frequency (Fig. 6b). We also measured the pair-pulse ratio as an indicator of the initial vesicular release probability.

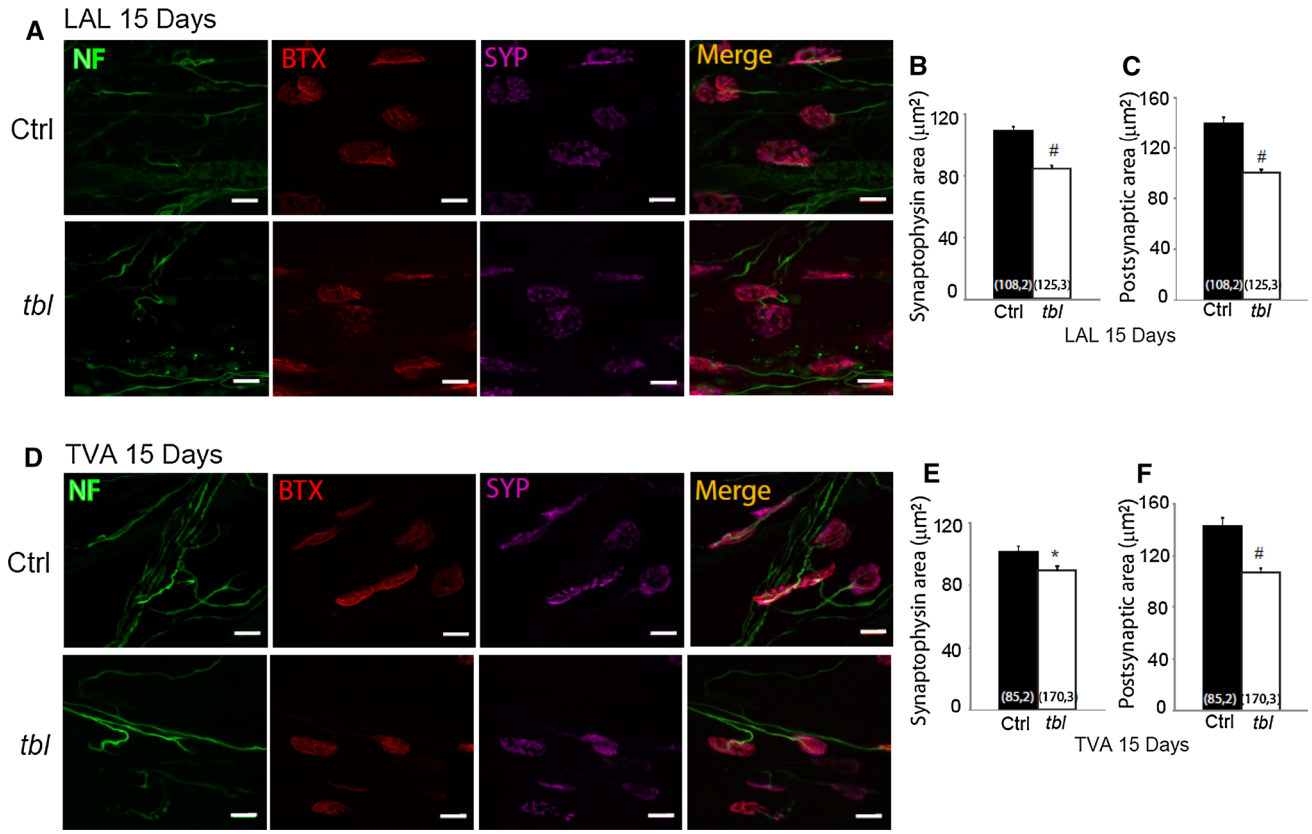

Fig. 4 SYP and BTX areas in motor terminals of *tbl* mice are smaller than in control littermates at P15 in fast- and slow-twitch muscle. Representative *en face* views of NMJs from the *LAL* (**a**) and *TVA* (**d**) muscle stained with BTX-Rho (*red*), anti-SYP (*magenta*) and NF (*green*). Images are Z-stack projections and the *scale bar* 10 µm. The mean synaptophysin areas were significantly smaller in mutants than in control terminals in both muscles: *LAL* (**b**) and *TVA* (**e**). The mean postsynaptic areas were significantly smaller in mutants than in control terminals, in both the *LAL* (**c**) and *TVA* (**f**) muscles: $^{*}p < 0.05$; $^{\#}p < 0.00005$ [(*n*, *N*), *n* number of NMJ, *N* number of mice]

No differences between controls and mutants were found at different frequencies (10–100 Hz: Fig. 6c) and thus short-term plasticity was well preserved in *tbl* mutant terminals despite the decrease in EPP amplitude and QC.

The readily releasable pool (RRP) is diminished in *tambaleante* mutant mice

The altered vesicular area and evoked release in *tbl* mutant mice might be due to a reduction in the number of vesicles available for release. We estimated the size of the RRP in *tbl* mutant mice through a functional assay of the representative EPP recording at 100 Hz during a 1 s stimulation (Fig. 7a). The mean RRP size was significantly smaller (by 35 %) in *tbl* mice (*tbl*: 900.7 ± 62.5; $n = 33$ terminals, 4 mice; Control: 1370.8 ± 106.5; $n = 23$ terminals, 3 mice, $p = 0.0003$: Fig. 7b), a decrease that may reflect a fall in the number of vesicles available (***n***) to be released or in the probability of release (**Pr**). Therefore, we estimated these parameters (see "Materials and methods") and while the vesicle release probability was not significantly different between control and *tbl* mice (*tbl*: 0.57 ± 0.03; Control: 0.55 ± 0.03, $p = 0.53$: Fig. 7c), the number of available vesicles was significantly lower in mutant terminals (*tbl*: 28.51 ± 2.49; Control: 41.37 ± 3.74, $p = 0.006$: Fig. 7c). Hence, the lower QC appeared to be due to a reduction in the RRP size.

Discussion

We show here that HERC1 E3 Ubiquitin Ligase fulfills an important role in maintaining normal evoked neurotransmitter release at the mouse NMJ. The alteration in HERC1 function present in *tambaleante* mice provokes a reduction in the number of vesicles available at these synapses. Furthermore, the motor dysfunction in these mice precedes the onset of the ataxic phenotype.

Our EMG measurements allow us to measure motor function in the mouse hind limb muscle (*MG*) in vivo and compare it with control littermates. Our results suggest that the mutation in the HERC1 E3 Ubiquitin Ligase (Gly483Glu

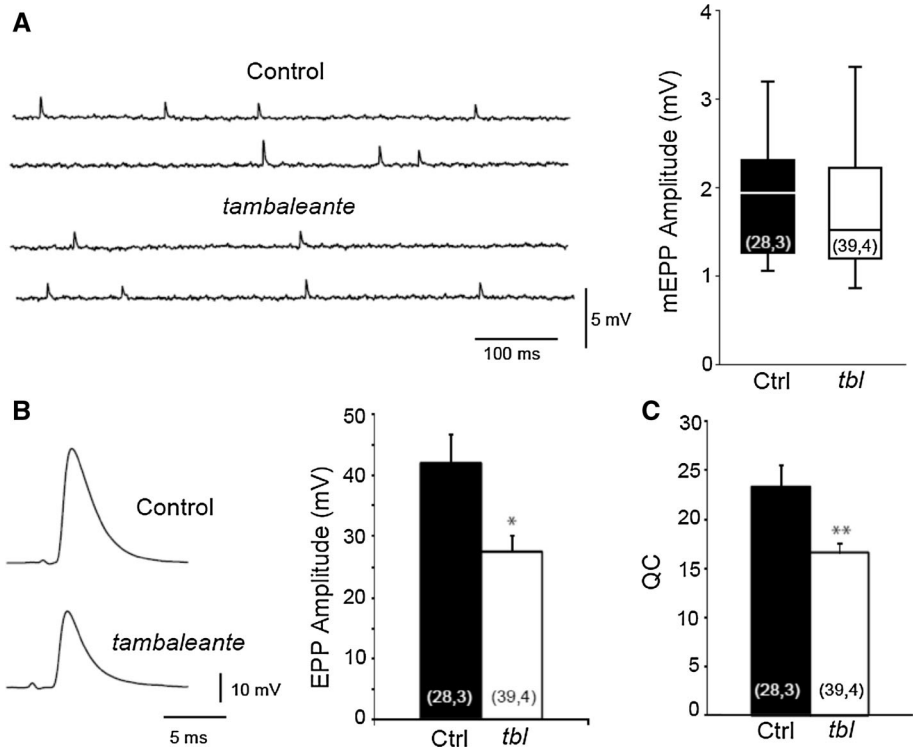

Fig. 5 Impaired evoked neurotransmitter release in *tbl* mutant mice. **a** Representative traces and median and interquartile range of mEPPs in control and mutant terminals. Representative EPP traces and mean EPP amplitudes (**b**) and mean quantum content (QC) (**c**) in control and *tbl* terminals: $*p < 0.05$; $**p < 0.005$ [(n, N), n number of fibers, N number of mice]

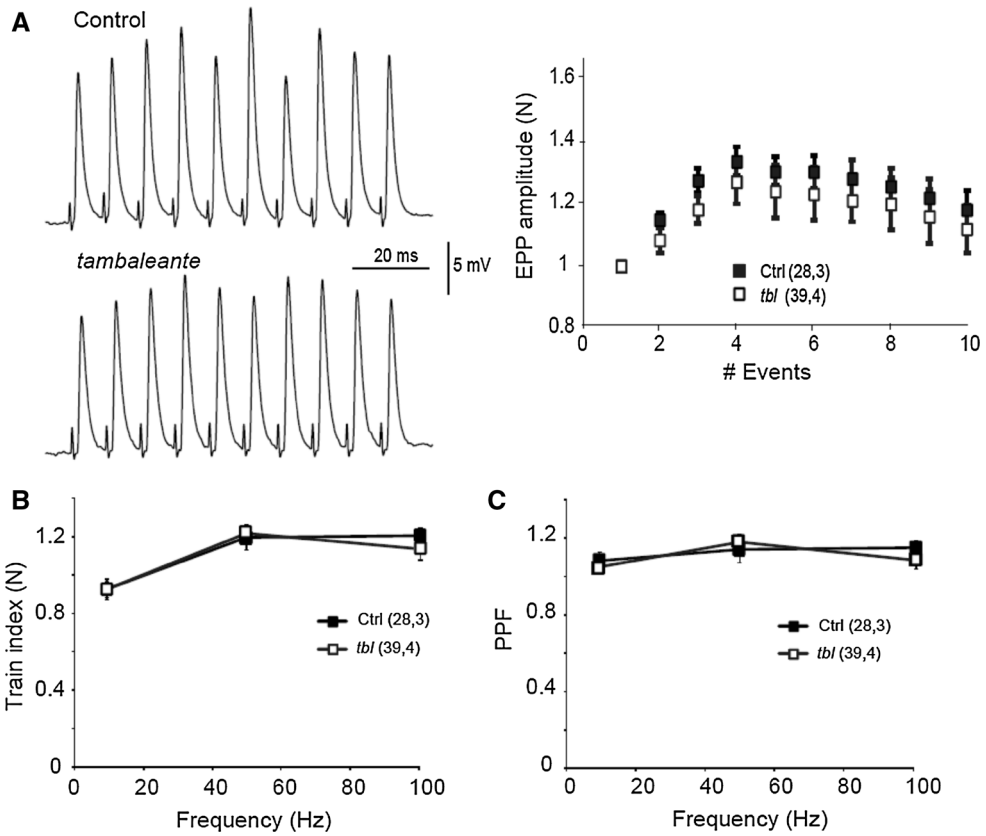

Fig. 6 Short-term plasticity is preserved in neuromuscular junctions in *tambaleante* mutant mice. **a** Representative traces in response to a train of stimuli at 100 Hz and EPP amplitude normalized to the first response. Train index at the end of the responses (**b**) and pair pulse facilitation (PPF) at all the frequencies of stimulation studied [(n, N), n number of fibers, N number of mice]

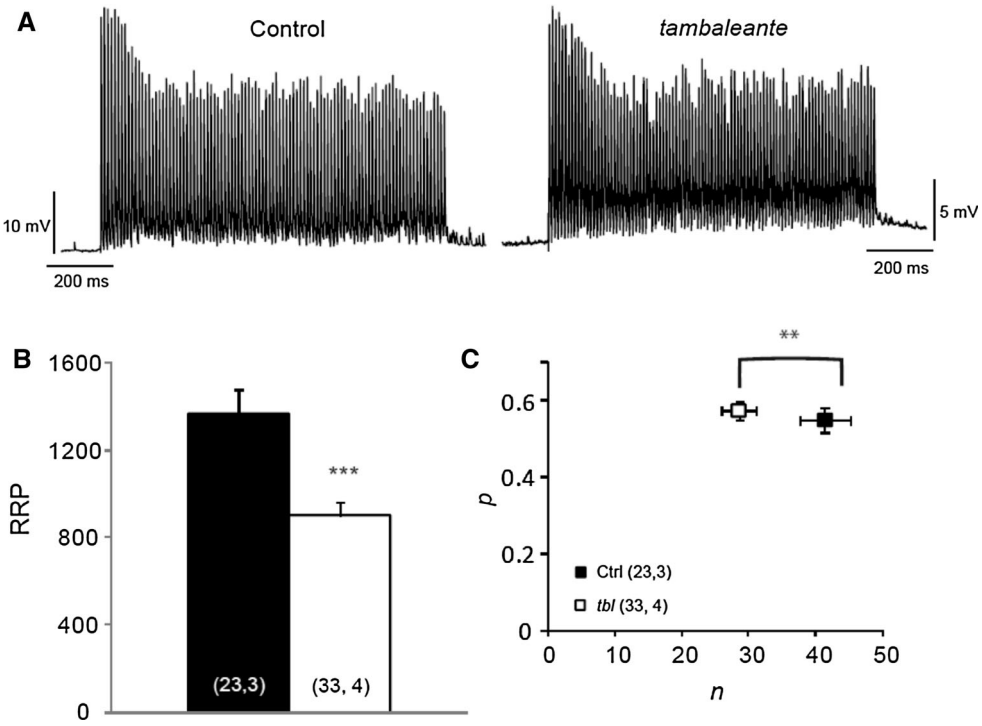

Fig. 7 The readily releasable pool (RRP) is decreased in *tambaleante* mutant mice. **a** Representative traces during a 100 Hz stimulation train of 1 s in a control and *tbl* mouse. **b** The mean RRP estimated in both groups. **c** *n* (number of occupied sites) and *p* (probability of release) estimated in control and *tbl* mice: $^{**}p < 0.005$; $^{***}p < 0.0005$ [(*n*, *N*), *n* number of fibers, *N* number of mice]

substitution) present in the *tbl* mice is responsible for the altered motor phenotype we found at P30, although interestingly this altered motor effect is evident before the onset of the ataxic phenotype. This phenomenon is not exclusive to *tbl* as there are other mouse models that exhibit motor impairment prior to the loss of PCs and the appearance of ataxia, such as: the *staggerer* mutant mice (functional loss of retinoid-related orphan receptor α—RORα-transcription factor); *rolling Nagoya* mice (mutation in the alpha1 subunit of the Cav2.1 channel); or the SCA1 conditional transgenic mice (a point mutation in ataxi-1) [33–36].

We detect motor dysfunction in these mutant mice at 1 month of age, while NMJ abnormalities in slow- and fast-twitch muscles were even evident at 2 weeks of age, such as smaller synaptic vesicles and postsynaptic area. The difference in the area measured between the mutant and wild-type mice could be due to a generalized problem during development, although at 15 days of age there was no significant difference in body weight between the two groups of mice. Defects in NMJ maturation precede age-depend motor dysfunction, as also observed in other mouse models where morphological problems associated with motor dysfunction appear prior to functional changes [30, 37]. Furthermore, other mice carrying mutations in proteins implicated in the ubiquitin–proteasome system also display motor impairment [5–8, 13]. Indeed, motor impairment and morphological changes at NMJs were also accompanied by deficits in neurotransmission. This is not surprising because there are many examples of mouse disease models with motor disorders associated with impaired neuromuscular transmission, such as spinal muscular atrophy, lateral amyotrophic sclerosis, and Huntington's disease [20, 24, 38–40]. Thus, these data support a model in which HERC1 plays a key role in the development and maintenance of mature NMJs.

The UPS is required for the rapid and precise control of the amount of proteins in neurons, some of which are essential for synaptic processes (reviewed by [1, 41, 42]). When a presynaptic terminal is activated, its complex molecular machinery drives the exocytosis of SVs, continuing the cycle with their endocytosis, recycling and refilling with neurotransmitters for a new round of release [43]. This process is tightly regulated by the activation and degradation of the proteins implicated, among other events [4, 41, 42]. In a Drosophila model, it was previously shown that proteasome inhibitors increase NMJ evoked release [44] and furthermore, proteasome inhibitors (clasto-lactacystin-lactone, epoxomicin or MG-132) augment the recycling pool in primary cultures of mouse hippocampal neurons, without affecting the probability of vesicle release [45]. Similarly, the probability of neurotransmitter release was not affected in NMJs from *tambaleante* mice, although we observed a decrease in EPP amplitude associated with a decrease in the RRP and number of vesicles available. Therefore, it is likely that the HERC1 Gly483Glu substitution in *tbl* mice has the opposite effect to that produced by proteasome inhibitors. In fact, the expression of the mutated HERC1 protein is greater in *tbl mice* than in

controls [15], suggesting that the increase in proteasomal activity could be sustained in *tbl* mice. Indeed, in mice carrying a loss-of-function USP14 (another UPS component, a deubuquitinase) there are fewer ubiquitinated proteins as well as less evoked release at the NMJ, supporting our hypothesis [13, 46, 47].

The mechanism by which HERC1 regulates neurotransmission remains unknown, although animal models with alterations in some UPS components present changes in the expression of proteins involved in the SV cycle, such as synaptophysin [48], SNAP25 [49], syntaxin [50], and MUNC13 [4]. Furthermore, recent studies have found that USP14 might have a different function to that of proteasomal catalytic activity [51, 52]. The same could occur with the E3-ligase-ubiquitin HERC1 and further studies will be necessary to determine the mechanism driving altered vesicle homeostasis in the *tambaleante* mutants, and how this alteration could participate in neurodegeneration.

In conclusion, our results show that HERC1 is essential for neurotransmitter release and vesicle homeostasis in NMJs. Although the exact mechanism involved in NMJ development and functional impairment is not known, our results invite us to hypothesize that the mutation of this UPS component could be implicated in motor neuron disease. Understanding the specific proteins involved in synaptic regulation will open new avenues for the treatment of these neurodegenerative diseases.

Acknowledgments We are grateful to Drs. Manel Santafe and Luis Miguel Real for their helpful comments and Dr. M. Sefton for editorial assistance. This work was supported by grants from MINECO JCI-2011-08888 (RR) and BFU2011-27207, and by the Fundación Ramón Areces (AMC).

References

1. Hegde AN, Upadhya SC (2007) The ubiquitin-proteasome pathway in health and disease of the nervous system. Trends Neurosci 30(11):587–595
2. van Tijn P, Hol EM, van Leeuwen FW, Fischer DF (2008) The neuronal ubiquitin-proteasome system: murine models and their neurological phenotype. Prog Neurobiol 85(2):176–193
3. Lu Z, Je HS, Young P, Gross J, Lu B, Feng G (2007) Regulation of synaptic growth and maturation by a synapse-associated E3 ubiquitin ligase at the neuromuscular junction. J Cell Biol 177(6):1077–1089
4. Tada H, Okano HJ, Takagi H, Shibata S, Yao I, Matsumoto M, Saiga T, Nakayama KI, Kashima H, Takahashi T, Setou M, Okano H (2010) Fbxo45, a novel ubiquitin ligase, regulates synaptic activity. J Biol Chem 285(6):3840–3849
5. Deng HX, Chen W, Hong ST, Boycott KM, Gorrie GH, Siddique N, Yang Y, Fecto F, Shi Y, Zhai H, Jiang H, Hirano M, Rampersaud E, Jansen GH, Donkervoort S, Bigio EH, Brooks BR, Ajroud K, Sufit RL, Haines JL, Mugnaini E, Pericak-Vance MA, Siddique T (2011) Mutations in UBQLN2 cause dominant X-linked juvenile and adult-onset ALS and ALS/dementia. Nature 477(7363):211–215
6. Dlamini N, Josifova DJ, Paine SM, Wraige E, Pitt M, Murphy AJ, King A, Buk S, Smith F, Abbs S, Sewry C, Jacques TS, Jungbluth H (2013) Clinical and neuropathological features of X-linked spinal muscular atrophy (SMAX2) associated with a novel mutation in the UBA1 gene. Neuromuscul Disord 23(5):391–398
7. Ramser J, Ahearn ME, Lenski C, Yariz KO, Hellebrand H, von Rhein M, Clark RD, Schmutzler RK, Lichtner P, Hoffman EP, Meindl A, Baumbach-Reardon L (2008) Rare missense and synonymous variants in UBE1 are associated with X-linked infantile spinal muscular atrophy. Am J Hum Genet 82(1):188–193
8. Rusmini P, Sau D, Crippa V, Palazzolo I, Simonini F, Onesto E, Martini L, Poletti A (2007) Aggregation and proteasome: the case of elongated polyglutamine aggregation in spinal and bulbar muscular atrophy. Neurobiol Aging 28(7):1099–1111
9. de Vrij FM, Fischer DF, van Leeuwen FW, Hol EM (2004) Protein quality control in Alzheimer's disease by the ubiquitin proteasome system. Prog Neurobiol 74(5):249–270
10. Rubinsztein DC (2006) The roles of intracellular protein-degradation pathways in neurodegeneration. Nature 443(7113):780–786
11. Upadhya SC, Hegde AN (2005) Ubiquitin-proteasome pathway components as therapeutic targets for CNS maladies. Curr Pharm Des 11(29):3807–3828
12. van Tijn P, Dennissen FJ, Gentier RJ, Hobo B, Hermes D, Steinbusch HW, Van Leeuwen FW, Fischer DF (2012) Mutant ubiquitin decreases amyloid beta plaque formation in a transgenic mouse model of Alzheimer's disease. Neurochem Int 61(5):739–748
13. Chen PC, Qin LN, Li XM, Walters BJ, Wilson JA, Mei L, Wilson SM (2009) The proteasome-associated deubiquitinating enzyme Usp14 is essential for the maintenance of synaptic ubiquitin levels and the development of neuromuscular junctions. J Neurosci 29(35):10909–10919
14. Kowalski JR, Dube H, Touroutine D, Rush KM, Goodwin PR, Carozza M, Didier Z, Francis MM, Juo P (2013) The Anaphase-Promoting Complex (APC) ubiquitin ligase regulates GABA transmission at the C. elegans neuromuscular junction. Mol Cell Neurosci 58C:62–75
15. Mashimo T, Hadjebi O, Amair-Pinedo F, Tsurumi T, Langa F, Serikawa T, Sotelo C, Guenet JL, Rosa JL (2009) Progressive Purkinje cell degeneration in tambaleante mutant mice is a consequence of a missense mutation in HERC1 E3 ubiquitin ligase. PLoS Genet 5(12):e1000784
16. Porras-Garcia ME, Ruiz R, Perez-Villegas EM, Armengol JA (2013) Motor learning of mice lacking cerebellar Purkinje cells. Front Neuroanat 7:4
17. Rossi F, Jankovski A, Sotelo C (1995) Target neuron controls the integrity of afferent axon phenotype: a study on the Purkinje cell-climbing fiber system in cerebellar mutant mice. J Neurosci 15(3 Pt 1):2040–2056
18. Wassef M, Sotelo C, Cholley B, Brehier A, Thomasset M (1987) Cerebellar mutations affecting the postnatal survival of Purkinje cells in the mouse disclose a longitudinal pattern of differentially sensitive cells. Dev Biol 124(2):379–389
19. Ruiz R, Lin J, Forgie A, Foletti D, Shelton D, Rosenthal A, Tabares L (2005) Treatment with trkC agonist antibodies delays disease progression in neuromuscular degeneration (nmd) mice. Hum Mol Genet 14(13):1825–1837
20. Ruiz R, Tabares L (2014) Neurotransmitter release in motor nerve terminals of a mouse model of mild spinal muscular atrophy. J Anat 224(1):74–84
21. Simon CM, Jablonka S, Ruiz R, Tabares L, Sendtner M (2010) Ciliary neurotrophic factor-induced sprouting preserves motor

function in a mouse model of mild spinal muscular atrophy. Hum Mol Genet 19(6):973–986
22. Ruiz R, Biea IA, Tabares L (2014) alpha-Synuclein A30P decreases neurodegeneration and increases synaptic vesicle release probability in CSPalpha-null mice. Neuropharmacology 76 Pt A:106–117
23. Ruiz R, Casanas JJ, Sudhof TC, Tabares L (2008) Cysteine string protein-alpha is essential for the high calcium sensitivity of exocytosis in a vertebrate synapse. Eur J Neurosci 27(12):3118–3131
24. Ruiz R, Casanas JJ, Torres-Benito L, Cano R, Tabares L (2010) Altered intracellular Ca2 + homeostasis in nerve terminals of severe spinal muscular atrophy mice. J Neurosci 30(3):849–857
25. McLachlan EM, Martin AR (1981) Non-linear summation of end-plate potentials in the frog and mouse. J Physiol 311:307–324
26. Ruiz R, Cano R, Casanas JJ, Gaffield MA, Betz WJ, Tabares L (2011) Active zones and the readily releasable pool of synaptic vesicles at the neuromuscular junction of the mouse. J Neurosci 31(6):2000–2008
27. Elmqvist D, Quastel DM (1965) A quantitative study of end-plate potentials in isolated human muscle. J Physiol 178(3):505–529
28. Yang L, Wang B, Long C, Wu G, Zheng H (2007) Increased asynchronous release and aberrant calcium channel activation in amyloid precursor protein deficient neuromuscular synapses. Neuroscience 149(4):768–778
29. Fontan-Lozano A, Suarez-Pereira I, Gonzalez-Forero D, Carrion AM (2011) The A-current modulates learning via NMDA receptors containing the NR2B subunit. PLoS One 6(9):e24915
30. Torres-Benito L, Neher MF, Cano R, Ruiz R, Tabares L (2011) SMN requirement for synaptic vesicle, active zone and microtubule postnatal organization in motor nerve terminals. PLoS One 6(10):e26164
31. Arnold AS, Gill J, Christe M, Ruiz R, McGuirk S, St-Pierre J, Tabares L, Handschin C (2014) Morphological and functional remodelling of the neuromuscular junction by skeletal muscle PGC-1alpha. Nat Commun 5:3569
32. Liu G, Tsien RW (1995) Properties of synaptic transmission at single hippocampal synaptic boutons. Nature 375(6530):404–408
33. Caston J, Delhaye-Bouchaud N, Mariani J (1995) Motor behavior of heterozygous staggerer mutant (+/sg) versus normal (+/+) mice during aging. Behav Brain Res 72(1–2):97–102
34. Clark HB, Burright EN, Yunis WS, Larson S, Wilcox C, Hartman B, Matilla A, Zoghbi HY, Orr HT (1997) Purkinje cell expression of a mutant allele of SCA1 in transgenic mice leads to disparate effects on motor behaviors, followed by a progressive cerebellar dysfunction and histological alterations. J Neurosci 17(19): 7385–7395
35. Takahashi E, Niimi K, Itakura C (2010) Neonatal motor functions in Cacna1a-mutant rolling Nagoya mice. Behav Brain Res 207(2):273–279
36. Takechi Y, Mieda T, Iizuka A, Toya S, Suto N, Takagishi K, Nakazato Y, Nakamura K, Hirai H (2013) Impairment of spinal motor neurons in spinocerebellar ataxia type 1-knock-in mice. Neurosci Lett 535:67–72
37. Sleigh JN, Grice SJ, Burgess RW, Talbot K, Cader MZ (2014) Neuromuscular junction maturation defects precede impaired lower motor neuron connectivity in Charcot-Marie-Tooth type 2D mice. Hum Mol Genet 23(10):2639–2650
38. Kong L, Wang X, Choe DW, Polley M, Burnett BG, Bosch-Marce M, Griffin JW, Rich MM, Sumner CJ (2009) Impaired synaptic vesicle release and immaturity of neuromuscular junctions in spinal muscular atrophy mice. J Neurosci 29(3):842–851
39. Rocha MC, Pousinha PA, Correia AM, Sebastiao AM, Ribeiro JA (2013) Early changes of neuromuscular transmission in the SOD1(G93A) mice model of ALS start long before motor symptoms onset. PLoS One 8(9):e73846
40. Rozas JL, Gomez-Sanchez L, Tomas-Zapico C, Lucas JJ, Fernandez-Chacon R (2011) Increased neurotransmitter release at the neuromuscular junction in a mouse model of polyglutamine disease. J Neurosci 31(3):1106–1113
41. DiAntonio A, Hicke L (2004) Ubiquitin-dependent regulation of the synapse. Annu Rev Neurosci 27:223–246
42. Kowalski JR, Juo P (2012) The role of deubiquitinating enzymes in synaptic function and nervous system diseases. Neural Plast 2012:892749
43. Sudhof TC (2004) The synaptic vesicle cycle. Annu Rev Neurosci 27:509–547
44. Speese SD, Trotta N, Rodesch CK, Aravamudan B, Broadie K (2003) The ubiquitin proteasome system acutely regulates presynaptic protein turnover and synaptic efficacy. Curr Biol 13(11):899–910
45. Willeumier K, Pulst SM, Schweizer FE (2006) Proteasome inhibition triggers activity-dependent increase in the size of the recycling vesicle pool in cultured hippocampal neurons. J Neurosci 26(44):11333–11341
46. Bhattacharyya BJ, Wilson SM, Jung H, Miller RJ (2012) Altered neurotransmitter release machinery in mice deficient for the deubiquitinating enzyme Usp14. Am J Physiol Cell Physiol 302(4):C698–C708
47. Chen PC, Bhattacharyya BJ, Hanna J, Minkel H, Wilson JA, Finley D, Miller RJ, Wilson SM (2011) Ubiquitin homeostasis is critical for synaptic development and function. J Neurosci 31(48):17505–17513
48. Wheeler TC, Chin LS, Li Y, Roudabush FL, Li L (2002) Regulation of synaptophysin degradation by mammalian homologues of seven in absentia. J Biol Chem 277(12):10273–10282
49. Ma Z, Portwood N, Foss A, Grill V, Bjorklund A (2005) Evidence that insulin secretion influences SNAP-25 through proteasomal activation. Biochem Biophys Res Commun 329(3):1118–1126
50. Chin LS, Vavalle JP, Li L (2002) Staring, a novel E3 ubiquitin-protein ligase that targets syntaxin 1 for degradation. J Biol Chem 277(38):35071–35079
51. Mukhopadhyay D, Riezman H (2007) Proteasome-independent functions of ubiquitin in endocytosis and signaling. Science 315(5809):201–205
52. Walters BJ, Hallengren JJ, Theile CS, Ploegh HL, Wilson SM, Dobrunz LE (2014) A catalytic independent function of the deubiquitinating enzyme USP14 regulates hippocampal synaptic short-term plasticity and vesicle number. J Physiol 592(Pt 4):571–586